Journal of Inflammation Research

Dovepress
open access to scientific and medical research

Open Access Full Text Article

ORIGINAL RESEARCH

Overexpression of Plakophilin2 Mitigates Capillary Leak Syndrome in Severe Acute Pancreatitis by Activating the p38/MAPK Signaling Pathway

Hui Liu[1,2], Xuan Xu[3], Ji Li[3], Zheyu Liu[1], Yuwen Xiong[1], Mengli Yue[4], Pi Liu[1]

[1]Department of Gastroenterology, The First Affiliated Hospital, Jiangxi Medical College, Nanchang University, Nanchang, People's Republic of China; [2]Gastroenterology Institute of Jiangxi Province, Nanchang, People's Republic of China; [3]Department of Gastroenterology, The People's Hospital of Longhua, Shenzhen, People's Republic of China; [4]Affiliated Longhua People's Hospital, The Third School of Clinical Medicine, Southern Medical University, Shenzhen, People's Republic of China

Correspondence: Pi Liu, Department of Gastroenterology, The First Affiliated Hospital, Jiangxi Medical College, Nanchang University, Nanchang, People's Republic of China, Tel +86-13507913736, Email liupi126@sina.com

Purpose: Capillary leak syndrome (CLS) is an intermediary phase between severe acute pancreatitis (SAP) and multiple organ failure. As a result, CLS is of clinical importance for enhancing the prognosis of SAP. Plakophilin2 (PKP2), an essential constituent of desmosomes, plays a critical role in promoting connections between epithelial cells. However, the function and mechanism of PKP2 in CLS in SAP are not clear at present.

Methods: We detected the expression of PKP2 in mice pancreatic tissue by transcriptome sequencing and bioinformatics analysis. PKP2 was overexpressed and knocked down to assess its influence on cell permeability, the cytoskeleton, tight junction molecules, cell adhesion junction molecules, and associated pathways.

Results: PKP2 expression was increased in the pancreatic tissues of SAP mice and human umbilical vein endothelial cells (HUVECs) after lipopolysaccharide (LPS) stimulation. PKP2 overexpression not only reduced endothelial cell permeability but also improved cytoskeleton relaxation in response to acute inflammatory stimulation. PKP2 overexpression increased levels of ZO-1, occludin, claudin1, β-catenin, and connexin43. The overexpression of PKP2 in LPS-induced HUVECs counteracted the inhibitory effect of SB203580 (a p38/MAPK signaling pathway inhibitor) on the p38/MAPK signaling pathway, thereby restoring the levels of ZO-1, β-catenin, and claudin1. Additionally, PKP2 suppression eliminated the enhanced levels of ZO-1, β-catenin, occludin, and claudin1 induced by dehydrocorydaline. We predicted that the upstream transcription factor PPARγregulates PKP2 expression, and our findings demonstrate that the PPARγactivator rosiglitazone significantly upregulates PKP2, whereas its antagonist GW9662 down-regulates PKP2. Administration of rosiglitazone significantly reduced the increase in HUVECs permeability stimulated by LPS. Conversely, PKP2 overexpression counteracted the GW9662-induced reduction in ZO-1, phosphorylated p38/p38, and claudin1.

Conclusion: The activation of the p38/MAPK signaling pathway by PKP2 mitigates CLS in SAP. PPARγactivator rosiglitazone can up-regulate PKP2. Overall, directing efforts toward PKP2 could prove to be a feasible treatment approach for effectively managing CLS in SAP.

Keywords: severe acute pancreatitis, plakophilin2, capillary leak syndrome, tight junction, p38/MAPK signaling pathway

Introduction

The global incidence of acute pancreatitis (AP), the most common gastrointestinal disorder requiring immediate hospitalization, is steadily increasing.[1,2] AP is characterized by inflammation of the pancreas, specifically in the exocrine region. AP can cause inflammation in nearby organs and throughout the body, leading to the death of pancreatic tissue and failure of many organs. Approximately 10–20% of patients with AP will experience SAP with systemic inflammatory response syndrome (SIRS).[3] The presence of either single organ failure or multiple organ failure (MOF), commonly referred to as multiple organ dysfunction syndrome,[4] is linked to a 40% to 50% risk of death.[5,6] CLS is a transitional stage of multi-organ dysfunction caused by SAP, mainly manifested as endothelial dysfunction.[7] Damage to the

Received: 15 January 2024
Accepted: 18 June 2024
Published: 26 June 2024

Graphical Abstract

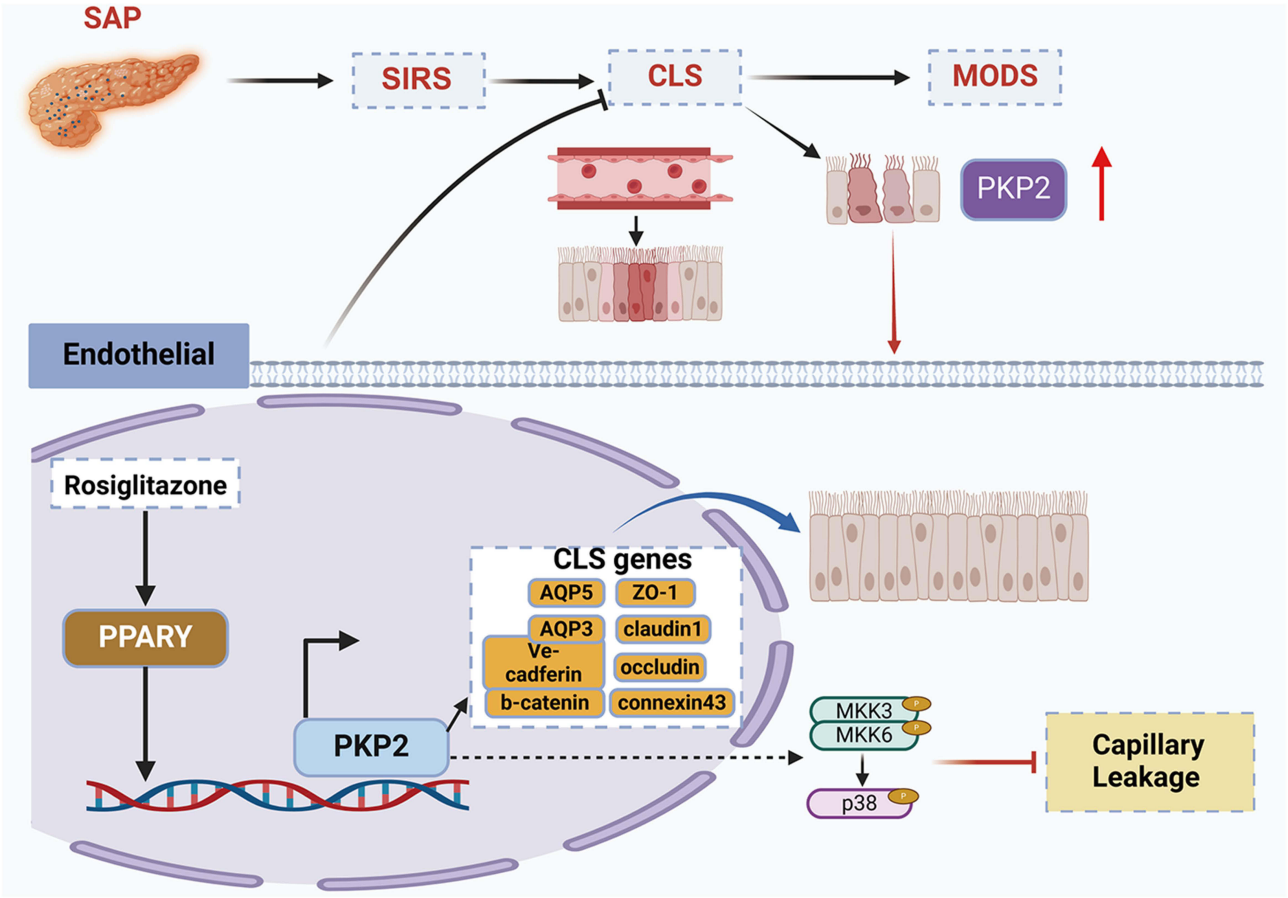

endothelial barrier in capillaries is primarily caused by the disruption of paracellular and transcellular pathways.[8] The paracellular system is linked to intercellular junctions whereas the transcellular pathway relies on aquaporins. CLS development causes widespread swelling of tissues and reduced blood volume,[9] which leads to inadequate blood supply to the pancreas, tissue death, and the release of pancreatic enzymes, such as trypsin, elastase, phospholipase A2, and activated neutrophils.[10] This process also increases the permeability of both pancreatic and systemic capillaries, establishing a harmful cycle that triggers the production of multiple cytokines, worsens SIRS, and ultimately contributes to MOF. The exact cause of SAP with CLS is unclear, and only a few therapeutic options are available. Hence, the molecular mechanisms that cause CLS in SAP must be elucidated to facilitate the development of drugs to prevent and treat this complication, and ultimately decrease its associated morbidity and death rates.

PKP2 is an essential component of desmosomes and a member of the plakophilin family. PKP2 plays a critical function in cell adhesion.[11] As the largest protein in the desmosomal plakophilin family, PKP2 possesses various armadillo repeats and is found in both cellular desmosomes and nuclei. PKP2 connects cadherin to the intermediate filaments of the cytoskeleton, which is not only responsible for intercellular connections, but also transmits cell signals through cell contact and regulates the electrophysiological and transcriptional pathways of cells.[12] The presence of the PKP2 mutation might result in the development of inherited arrhythmogenic right ventricular cardiomyopathy (ARVC).[13] This condition is characterized by the abnormal growth of fibrofatty tissue in the right ventricle, the occurrence of malignant ventricular arrhythmias, and a significantly elevated risk of sudden death.[14] Studies have shown damage to the nuclear membranes in the cardiomyocytes of the right ventricles of patients with ARVC and in the hearts of PKP2 mutant

mice. Loss of PKP2 leads to DNA damage and oxidative stress, which in turn results in the downregulation of proteins associated with the electron transport chain.[15] A separate investigation revealed that the removal of PKP2, specifically from cardiac cells, increases the expression of specific RNA molecules linked to inflammatory and immune responses. These findings suggest that adult cardiomyocyte PKP2 may play a role in controlling the production of inflammatory substances. Thus, suppressing the inflammatory response serves as a potential treatment strategy for ARVC.[16] According to various studies, PKP2 and the gap junction protein connexin43 combine to form a protein complex at the desmosome junction. This complex plays a crucial role in precisely positioning the tight junction proteins, occludin and zonula occludens-1(ZO-1), which are responsible for regulating intercellular adhesion.[17] PKP2 can directly regulate the focal adhesion, diffusion, and migration of keratinocytes by controlling the small GTPase, RhoA, and β1 integrin.[18] When PKP2 is knocked out, the absence of desmoplakin expression alters the conversion of growth factor β1 and triggers the activation of the p38 mitogen-activated protein kinase (MAPK) signaling pathway, leading to a notable increase in pro-fibrotic interleukin-1α and Ccl12 mRNA expression.[19] Activation of the muscarinic acetylcholine receptor M3 promotes inflammation and necrosis through the p38/miR-31-5p/RIP3 signaling pathway in L-arginine-induced SAP.[20] Currently, information on the involvement and mechanism of PKP2 in SAP is lacking. Further, whether PKP2 affects CLS in SAP through the p38/MAPK signaling pathway remains uncertain.

CLS primarily functions through paracellular and transcellular pathways. The paracellular pathway is related to intercellular communication whereas the transcellular pathway involves aquaporins.[8,21] The paracellular route predominantly depends on intercellular connections, including tight, gap, and adhesive junctions.[22] Tight junctions are composed of a claudin protein family, members of the connection-related molecules (JAM) family, cytoplasm-junction proteins (mainly ZO-1), occludin. ZO-1 plays a crucial role in controlling the permeability of blood vessels. Increasing the expression of ZO-1 can protect the barrier function of endothelial cells, mitigating damage induced by inflammatory factors.[23] Adhesion junctions are an important part of the cellular endothelial barrier, especially vascular endothelial VE-cadherin, which acts as the main adhesion receptor in endothelial adhesion junctions.[24] The transmembrane protein VE-Cadherin establishes direct intercellular connections between adjacent cells via its extracellular domain, while its intracellular domain associates with the cytoskeleton through catenin, thereby forming cell adhesion junctions. The catenin family includes p-120 catenin, β-catenin, γ-catenin, α-catenin, and various subtypes, each of which has specific functions in adhesion. According to Chen et al[25] increasing the stability of the VE-cadherin/β-catenin complex in endothelial cells can protect the integrity of the vascular endothelial barrier and prevent inflammation. The gap junction consists of two neighboring channels created by connexin semi-channels, which enable the fast transport of substances. In humans, connexin acts as the basic component of gap junctions with 20 known subtypes. Among these, connexin43 plays a vital role in facilitating vascular permeability.[26] Zhao et al[27] demonstrated that abnormal activation of the RhoA/ROCK1/pMLC signaling pathway alters the expression and localization of connexin43, leading to increased vascular permeability and dysfunction in vascular endothelial cells. Moreover, other studies have revealed that changes in the expression of connexin43 may play a role in the progression of chronic pancreatitis.[28] Nevertheless, the precise function of connexin43 in SAP remains unclear. Aquaporins in the transcellular pathway are vital to the pathways involved in the regulation of vascular endothelial permeability.[29] Zhang et al[30] found that reducing AQP3 expression increases the permeability of vascular endothelial cells. According to Jiang et al[31] the p38/MAPK signaling pathway can increase the expression of claudin3 and occludin. Moreover, Zhang et al[32] revealed that blocking the PI3K/AKT and p38/MAPK signaling pathways results in a reduction in tight junction proteins (ZO-1, occludin, claudin1) and AQP3. Based on previous research, activation of the ERK/p38 MAPK signaling pathway might cause an increase in the expression of the aquaporin-5 (AQP5).[33] However, whether PKP2 plays a role in the regulation of CLS in SAP remains uncertain. Moreover, the specific function of PKP2 in preventing SAP by regulating the p38/MAPK signaling pathway to increase the permeability of endothelial cells is not fully understood.

In our study, the expression of PKP2 was found to be significantly upregulated in the pancreatic tissue of mice with CLS in SAP and in the pancreatic acinus cells of cerulein-induced mice, indicating a potential role for PKP2 in SAP pathogenesis, either by exacerbating disease progression or mitigating disease severity. We generated a plasmid to overexpress PKP2 and conducted a knockdown experiment to examine the role and molecular mechanism of CLS in SAP. In an HUVEC model of acute inflammation induced by LPS, the increased expression of PKP2 resulted in

a decrease in the permeability of endothelial cells and improved the degree of endothelial cytoskeleton porosity. In contrast, a decrease in PKP2 levels led to an increase in the permeability of endothelial cells, which caused an increase in leakage and a higher level of porosity in the cytoskeleton. These findings indicate that PKP2 has a defensive effect on SAP. The subsequent investigation confirmed that PKP2 mitigates CLS in SAP by activating the p38/MAPK signaling pathway through rescue experiments. The PPARγactivator rosiglitazone protects SAP by upregating PKP2. Overall, PKP2 is markedly involved in the development of CLS in SAP and could serve as a new therapeutic target.

Materials and Methods

Animals

Wild-type male C57BL/6 mice were obtained from Beijing Spiff Biotechnology Co. Ltd. (Beijing, China). After 12 h of fasting, the mice were intraperitoneally administered 100 μg/kg of cerulein (HY-A0190, MCE). This process was repeated 10 times, with each injection spaced 1 h apart. On the tenth administration, 5 mg/kg of LPS (L8880, Solarbio) was injected into the peritoneal cavity. Mice in the control group were intraperitoneally administered an equivalent amount of normal saline. Mice had unrestricted access to food and sterile water. After 24 hours, the mice were euthanized by cervical dislocation. Pancreatic tissue, lung tissue, and blood were collected for analysis. A segment of the pancreas and lung tissue was preserved in 4% paraformaldehyde, and the remaining tissues were immediately frozen using liquid nitrogen and stored at −80 °C. Serum was obtained by centrifuging blood at 3000 × g for 10 min. Subsequently, the samples were stored at −80 °C.

Biochemical Detection and Enzyme Linked Immunosorbent Assay

An automated biochemical analyzer was used to measure the levels of serum amylase and lipase while Enzyme Linked Immunosorbent Assay (ELISA) was conducted to determine the levels of IL-6, Il-1β, and TNF-α in the serum.

Hematoxylin Eosin Staining and Immunohistochemistry

Paraffin-embedded pancreatic and lung tissues were stained with hematoxylin and eosin and observed using an optical microscope. To assess tissue damage in the pancreas and lungs, a sample of 10 random fields was collected by a minimum of two expert pathologists.[34,35] Immunohistochemical examination was then conducted using paraffin slices of pancreatic tissue to evaluate the expression of PKP2.

Evans Blue Test and Wet-Dry Weight Ratio Measurement

Evans blue stain solution (G1810, Solarbio) was intravenously administered to mice and allowed to circulate throughout the body for 2 h. The mouse heart was subsequently perfused until clear fluid drained from the right atrium. The pancreatic and lung tissues were obtained and fixed in formamide 3mL (HY-Y0842, MCE). After 48 h of incubation at 70 °C, the mixture was centrifuged at 1000 rpm for 5 min. The concentration of Evans Blue (EB) in the pancreatic and lung tissues was subsequently quantified by measuring the optical density (OD) at 610 nm using enzyme labeling equipment. The wet-dry weight ratio of the tissue was determined following a 72-hour drying period at 70 °C.

Cell Culture and Treatment

We cultured 266–6 cells (mouse acinar cell line, ATCC, USA) in RPMI 1640 medium supplemented with 10% fetal bovine serum. Human umbilical vein endothelial cells (HUVECs, ATCC, USA) were cultured in Dulbecco's modified Eagle medium (DMEM) supplemented with 10% fetal bovine serum. Human PKP2 (pCDH-CMV-HomoPKP2-EF1-copGFP-T2A-Puro) plasmid and control plasmid were procured from IGEBio (Guangzhou, China). Human siPKP2 mRNA (50 nM) was synthesized by Gemma Pharma (Shanghai, China) and transfected into HUVECs using the Lipofectamine 3000 reagent (Thermo Fisher, USA). 24 hours after transfection of PKP2 plasmid, HUVECs were treated with PPARγ agonist Rosiglitazone (10uM, HY-17386, MCE) and PPARγ antagonist GW9662 (10uM, HY-16578, MCE) 2 hours prior. Subsequently, the cells were incubated with LPS at a concentration of 1.0 μg/mL for 24 hours. At 24 h after transfection with siPKP2, 1 μM of the p38/MAPK activator, dehydrocorydaline (HY-N0674, MCE), and 10 μM of the p38/MAPK inhibitor, SB203580 (HY-10256, MCE), were

administered. HUVECs were added 30 min and 1 h earlier, respectively. After 24 h of stimulation, 1.0 μg/mL of LPS was added to the culture.

Fluorescent Yellow Test and Ghost Pen Cyclic Peptide Test

After transfection, the cells were stimulated with 1.0 μg/mL of LPS for 24 h and subsequently inoculated into transwell chambers. The upper part was supplemented with 100 μL of medium-diluted fluorescein solution (0.1 mg/mL) (HY-D0251, MCE), while the lower part was supplemented with 600 μL of serum-free DMEM. After 2 h of incubation, a 100μL aliquot of the lower layer from each transwell cell was extracted, and the fluorescence absorbance was measured using a multifunctional fluorescent enzyme spectrometer. The excitation wavelength was set at 480nm, while the emission wavelength was set at 520nm. Subsequently, the cells were inoculated into confocal dishes, fixed with 4% formaldehyde, and stained with TRITC Phalloidin (CA1610, Solarbio), a phalloidin solution diluted to 100 nM with Phosphate Buffer Saline (PBS). Finally, 4',6-diamidino-2-phenylindole (DAPI) (C1005, Beyotime) was used for nuclear staining and observation of the cytoskeleton under a fluorescence microscope.

Western Blotting Experiment

After protein extraction using radio immunoprecipitation assay (RIPA) lysis buffer containing protease and phosphatase inhibitors, the protein concentration was determined using a bicinchoninic acid kit (P0012S, Beyotime) to adjust for equal amounts of protein. Sodium dodecyl sulfate-polyacrylamide gel electrophoresis (SDS-PAGE) was performed and the separated proteins were transferred onto a polyvinylidene fluoride membrane (IPVH00010, Millipore). The membrane was sealed with 5% TBS-T Buffer skim milk and incubated overnight at 4 °C with the following primary antibodies: glyceraldehyde-3-phosphate dehydrogenase (GAPDH) (1:2000 dilution, 60004-1-Ig, Proteintech), PKP2 (1:1000 dilution, sc-393711, Santa Cruz), ZO-1 (1:500 dilution, AF5145, Affinity), β-catenin (1:1000 dilution, sc-7963, Santa Cruz), occludin (1:2000 dilution, 27260-1-AP, Proteintech), claudin 1 (28674 -AP, Proteintech), VE-cadherin (AF6265, Affinity), p38 (#8690 Cell Signaling Technology), and p-p38 (#45111 Cell Signaling Technology). Subsequently, the membranes were washed thrice with TBST for 10 min per wash and incubated with an anti-rabbit secondary antibody (PR30011 Proteintech) or anti-mouse secondary antibody (PR30012 Proteintech) at 37°C on a shaker for 1 h. Finally, the samples were exposed to a supersensitive chemiluminescent substrate. Quantitative analysis was performed using ImageJ software.

Quantitative Real Time Polymerase Chain Reaction

We extracted RNA using the classical Trizol method. cDNA synthesis was performed according to the instructions of Hifair® III 1st Strand cDNA Synthesis SuperMix for quantitative real time polymerase chain reaction (qRT-PCR) (11141ES60, Yeasen). Amplification was carried out using Hieff UNICON® Universal Blue qPCR SYBR Green Master Mix (11184ES08, Yeasen). For specific primer sequence information, see supplementary materials (Table S1). The primers were synthesized by Sangon Biotech (Shanghai, China). Finally, the relative mRNA expression level was calculated using the ΔΔCt method.

Statistical Analysis

Data are presented as mean ± standard deviation (SD). The data must undergo normality testing before analysis. For datasets that follow a normal distribution, a two-tailed Student's *t*-test was employed for comparing between two groups, while univariate analysis was used for comparing between more than two groups. Multiple comparisons were conducted in the univariate analysis to compare the two groups. Statistical analyses were performed using the Prism software (version 9.0; GraphPad Software, Inc). Statistical significance was set at $p < 0.05$.

Results

Successful Modeling of SAP with CLS

The assessment of inflammation in mice revealed elevated levels of amylase, lipase, IL-6, IL-1β, and TNF-α in SAP mice compared to the control group as indicated by serum biochemical and ELISA tests (Figure 1A and B). In addition, the

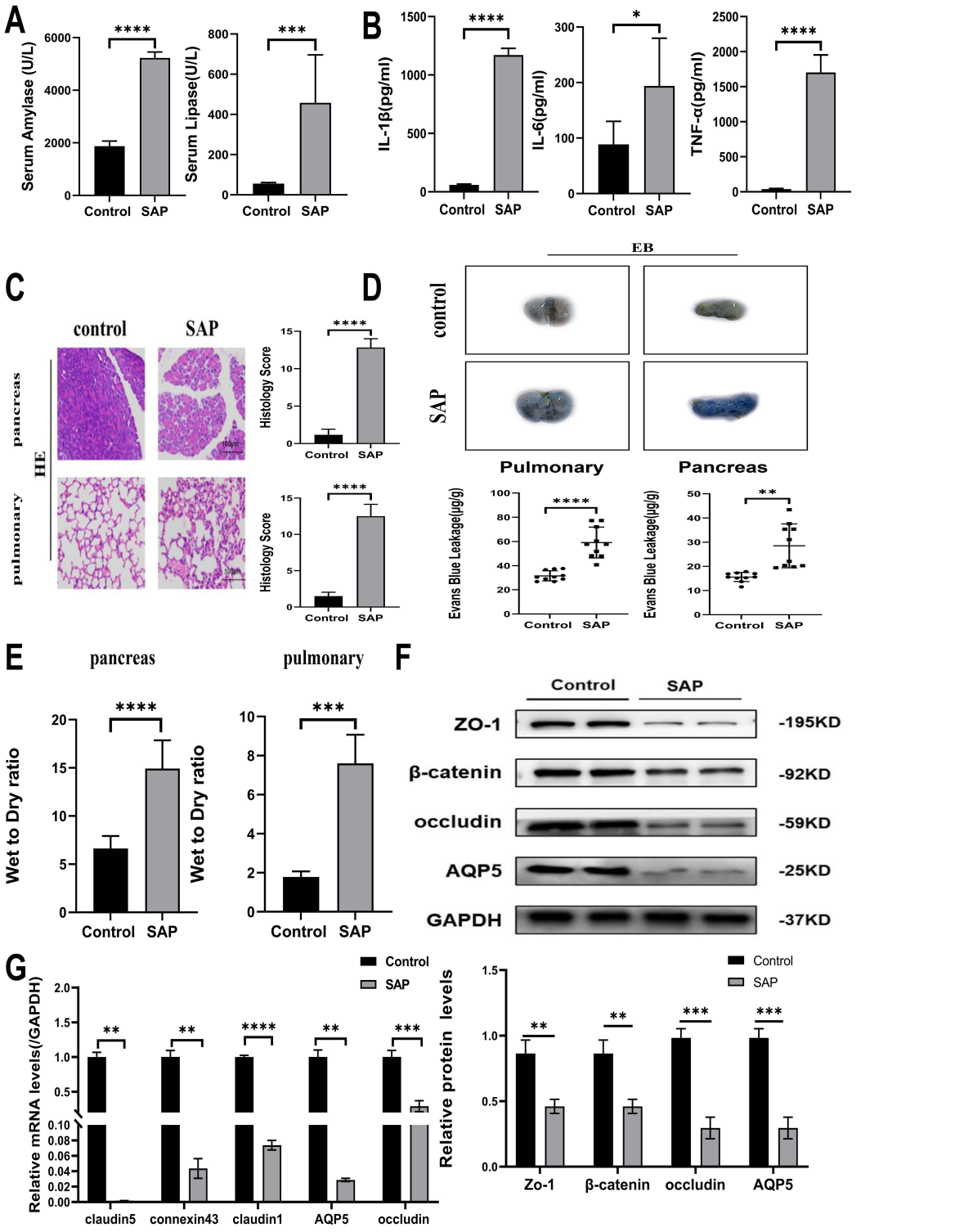

Figure 1 Cerulein combined with lipopolysaccharide-induced capillary leakage in SAP mice. (**A**) Serum amylase levels and lipase activity were measured in the control and SAP groups (n = 12/group). The mortality rate in each group was 0% (representative of three independent experiments). (**B**) The levels of serum inflammatory cytokines IL-6, IL-1β, and TNF-α were measured in both the control group and the SAP group (n = 12/group; data represent the results of three independent experiments). (**C**) Representative histological H&E staining maps (n = 6/group) and pathological scores of the pancreas and lung tissues were obtained for each group (n = 6/group; data represent the results of three independent experiments). Scale = 100 μm. (**D**) Representative Evans blue leakage maps of the pancreas and lung tissues were generated for each group (n = 6/group) and then quantitatively analyzed (data represent the results of three independent experiments). (**E**) Wet-dry weight ratios of the pancreas and lung tissues were determined for both groups (n = 6/group; data represent the results of three independent experiments). (**F**) Protein levels of pancreatic ZO-1, β-catenin, occludin, and AQP5 in the control and SAP groups were examined and quantitative analysis (data represent the results of three independent experiments). (**G**) mRNA levels of pancreatic claudin5, connexin43, claudin1, AQP5, and occludin in the control and SAP groups were determined (data represent the results of three independent experiments). GAPDH was used as a control. *p < 0.05, **p < 0.01, ***p < 0.001, ****p < 0.0001.

mRNA levels of IL-1β and TNF-α were increased in the pancreas (Figure S1). The Hematoxylin and eosin staining analysis revealed that mice in the SAP group exhibited pancreatic tissue structural destruction, necrosis, extensive infiltration of inflammatory cells, rupture and thickening of alveolar walls, alveolar hemorrhage, as well as inflammatory cell infiltration when compared to the control group (Figure 1C). The Evans blue experiment demonstrated that the leakage of Evans blue in pancreatic tissue and lung tissue of mice in the SAP group exhibited a significant increase when compared to the control group (Figure 1D). The wet-dry weight ratio of pancreas and lung tissue in the SAP group was found to be higher compared to the control group, indicating the presence of edema in both tissues (Figure 1E). Compared to the control group, Western blotting revealed a significant decrease in protein expression levels of ZO-1, β-catenin, occludin, and AQP5 in the SAP group (Figure 1F). Additionally, mRNA levels of claudin5, connexin43, claudin1, AQP5, and occludin were found to be decreased (Figure 1G). Collectively, CLS was found to occur with SAP.

PKP2 Expression is Upregulated in SAP Mice

The SAP mice model was established in C57BL/6J mice through continuous intraperitoneal administration of cerulein combined with lipopolysaccharide. The transcriptomic analysis of RNA-Seq data was conducted to identify novel genes associated with CLS, revealing an up-regulation of PKP2 expression in the SAP group compared to the control group, as demonstrated by volcanic and heat maps (Figure 2A). Gene enrichment and KEGG pathway analyses revealed that SAP plays a role in controlling adhesion molecules (Figure 2B). KEGG analysis also indicated that SAP is linked to adhesion, tight junctions, and gap junctions (Figure 2B). Immunohistochemical staining was performed to ascertain the expression level of PKP2 in the pancreas. Significant upregulation of PKP2 expression was observed in the vascular endothelial cells of the pancreatic tissue in SAP mice (Figure 2C). The protein and mRNA levels of PKP2 were significantly elevated as detected by Western blotting and qRT-PCR (Figure 2D). To examine the influence of PKP2 on the capillary endothelium, an acute inflammation model was established by inducing HUVECs with LPS. Western blot analysis revealed a notable reduction in the expression levels of ZO-1, VE-cadherin, β-catenin, occludin, and claudin1 after LPS stimulation. Conversely, the expression of PKP2 increased (Figure 2E). The mRNA expression levels of the inflammatory cytokines, IL-1β, TNF-α, and IL-6, were elevated after LPS stimulation (Figure 2F). Examination of gene expression in mouse pancreatic acinus cells revealed outcomes comparable to those of the in vivo investigation. By administering cerulein to stimulate 266–6 cells and determining the ideal concentration for stimulation (Figure S2), we discovered that the mRNA levels of the inflammatory markers, IL-1β, TNF-α, and IL-6, increased, and PKP2 expression was upregulated (Figure 2G). The above findings suggest an upregulation of PKP2 expression following CLS in SAP; however, further studies are needed to elucidate its precise role in this process.

Overexpression of PKP2 Can Reduce CLS to Protect SAP

To investigate the function of PKP2. The PKP2 overexpression plasmid was constructed and subsequently validated by WB (Figure 3A). Overexpression of PKP2 in HUVECs revealed its involvement in endothelial cell connection pathways. When transfection of PKP2 plasmid interfered with the HUVECs model of LPS-induced acute inflammation, qRT-PCR detection showed up-regulated mRNA expression of water channel genes AQP3 and AQP5 (Figure 3B), and up-regulated mRNA expression of tight junction genes claudin1 and occludin (Figure 3C). The expression of the adhesion junction gene ve-cadherin mRNA was also up-regulated (Figure 3D). Subsequently, the fluorescence yellow assay was employed to measure endothelial cell permeability, revealing that overexpression of PKP2 significantly reduced cell permeability during acute inflammation (Figure 3E). Additionally, Rhodamine staining also showed that overexpression of PKP2 improved the arrangement and morphology of F-actin in living cell filaments (Figure 3F). Similarly, Western blot analysis revealed that PKP2 overexpression upregulated the ZO-1, β-catenin, occludin, connexin43, and claudin1 proteins during acute inflammation (Figure 3G). Immunofluorescence confirmed an increase in claudin1 expression upon PKP2 overexpression (Figure 3H). Overall, PKP2 overexpression was found to ameliorate cell junction disorders caused by acute inflammation.

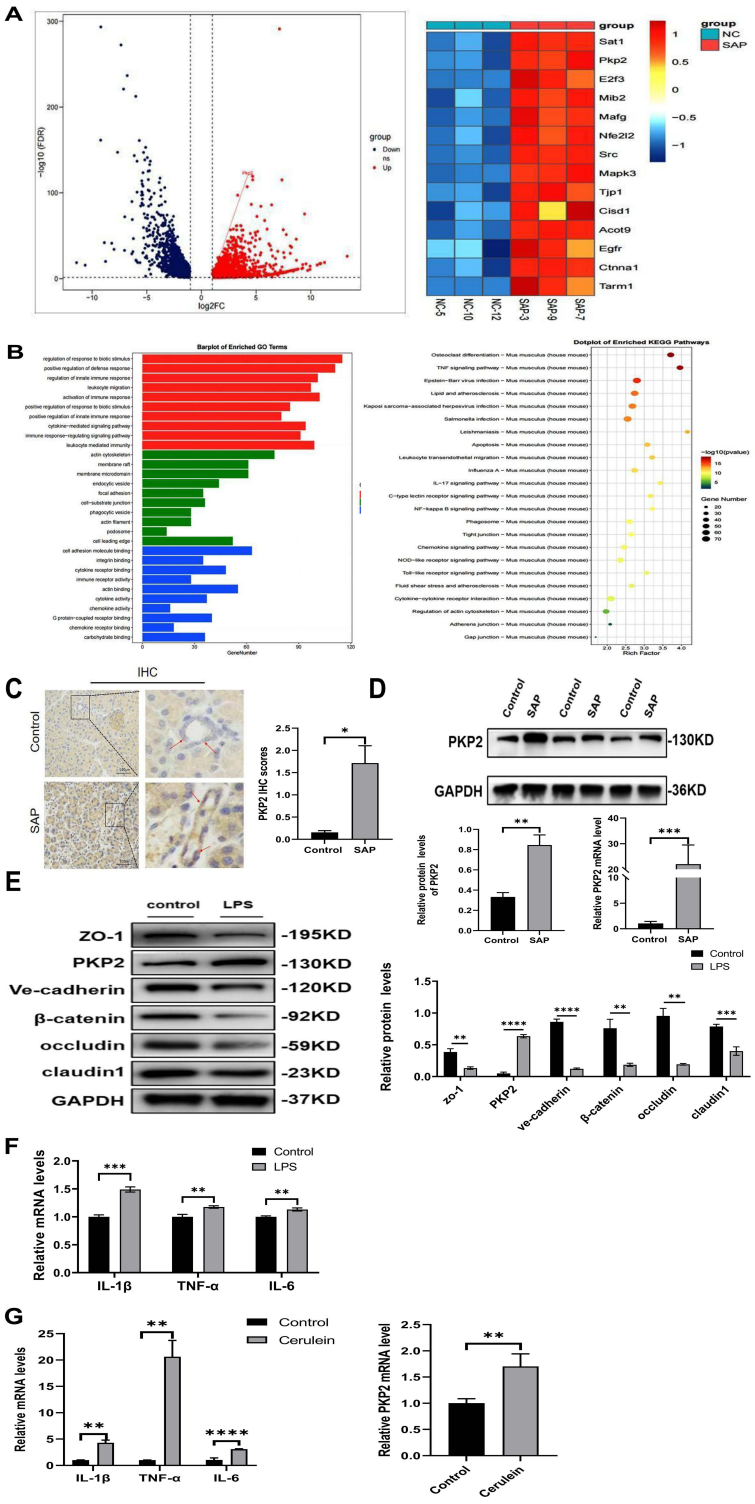

Figure 2 Transcriptomics of SAP mice and up-regulation of PKP2 expression in SAP mice. (**A** and **B**) Scatter plots and heat maps of RNA-seq data from the pancreas of mice in the control group and SAP group (n = 3/group) revealed an up-regulation of PKP2 expression in the SAP group compared to the control group (**A**), along with differential gene GO enrichment analysis and KEGG pathway enrichment analysis conducted on both groups (**B**). (**C**) Immunohistochemical staining of PKP2 in the pancreatic vascular endothelium was conducted using each group of mice (n = 6/group; data represent the results of three independent experiments). Scale = 100 μm. (**D**) The protein and mRNA levels of PKP2 in the pancreas of mice were measured in both the control group and SAP group, followed by quantitative analysis (n = 6/group; data represent the results of three independent experiments). (**E**) The protein levels and quantitative analysis of PKP2, ZO-1, Ve-cadherin, β-catenin, occludin, and claudin1 were assessed in HUVECs from both the control group and the LPS group (data represent the results of three independent experiments). The GAPDH protein was utilized as a control in both experiments (**D** and **E**). (**F**) qRT-PCR was performed to determine the mRNA levels of the inflammatory cytokines, IL-1β, TNF-α, and IL-6, after LPS stimulation (data represent the results of three independent experiments). (**G**) mRNA levels of PKP2, IL-1β, TNF-α, and IL-6 were determined in control and cerulein-treated 266–6 cells (data represent the results of three independent experiments). *p < 0.05, **p < 0.01, ***p < 0.001, ****p < 0.0001.

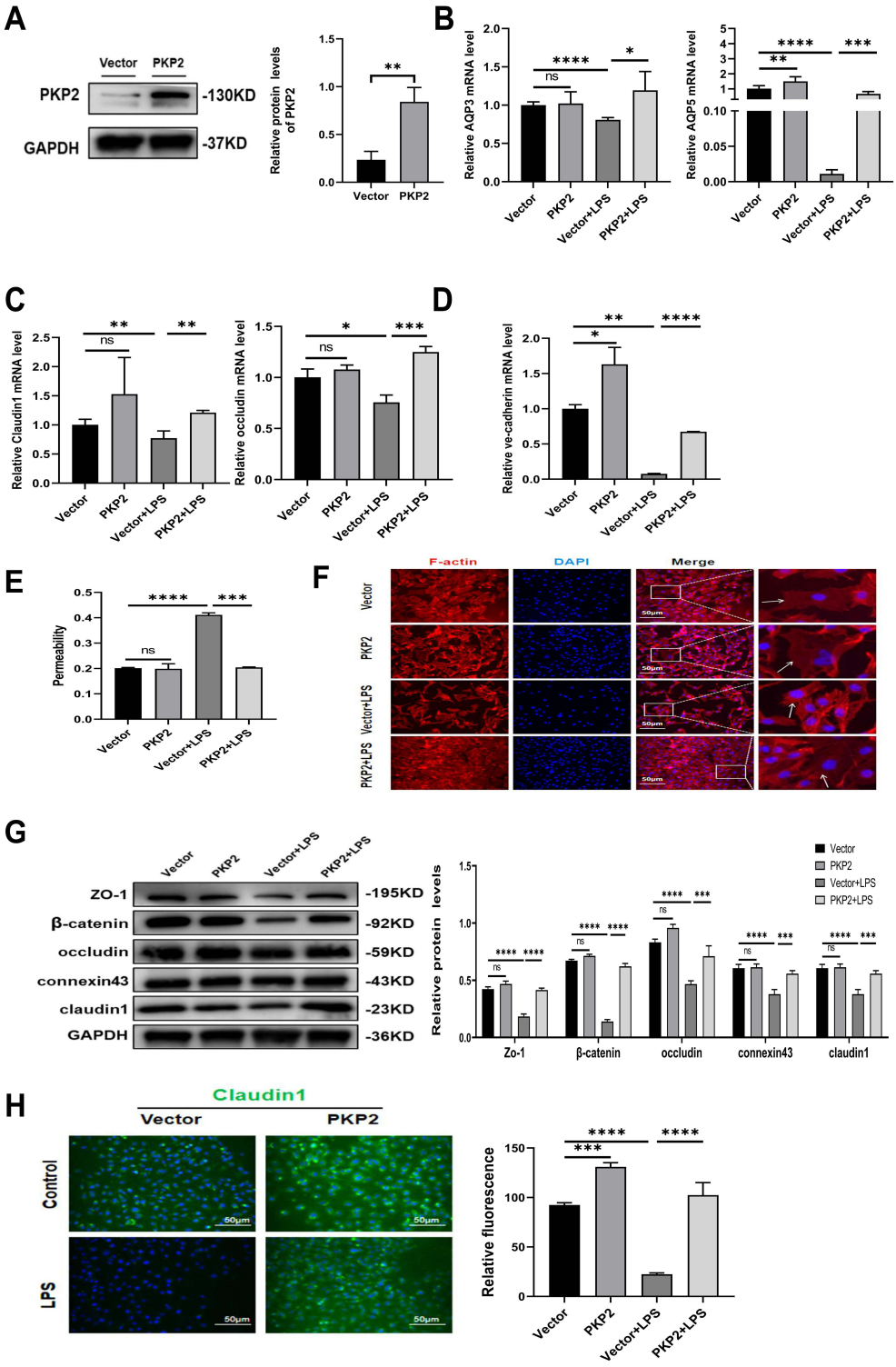

Figure 3 Overexpression of PKP2 improved CLS associated with acute inflammation. (**A**) Successful verification of the overexpression of the PKP2 protein was achieved (data represent the results of three independent experiments). (**B**–**D**) The mRNA expression levels of AQP3, AQP5, claudin1, occludin, and ve-cadherin in HUVECs overexpressing PKP2 and stimulated by LPS demonstrated that PKP2 overexpression upregulated the expression of CLS-related molecular genes (data represent the results of three independent experiments). (**E**) PKP2 overexpression attenuates the permeability of HUVECs during acute inflammation (data represent the results of three independent experiments). (**F**) PKP2 overexpression ameliorates LPS-induced cytoskeleton disorder in HUVECs (data represent the results of three independent experiments). (**G**) Increased protein levels of ZO-1, β-catenin, occludin, connexin43, and claudin1 were observed in HUVECs with acute inflammation upon PKP2 overexpression and quantitative analysis (representative of three independent experiments). (**H**) Immunofluorescence analysis demonstrating the upregulation of claudin1 expression due to PKP2 overexpression in HUVECs with acute inflammation (data represent the results of three independent experiments). *p < 0.05, **p < 0.01, ***p < 0.001, ****p < 0.0001; ns p > 0.05.

https://doi.org/10.2147/JIR.S459449 DovePress

Knocking Down PKP2 Increases the Degree of CLS

Instead, to study the function of knocking down PKP2. We constructed the PKP2 interfering RNA fragment and verified it successfully by WB and qRT-PCR (Figure 4A). Downregulation of PKP2 in HUVECs led to increased breakdown of intercellular connections. After transfection of siPKP2, interference with the HUVECs model of LPS-induced acute inflammation resulted in a significant down-regulation of mRNA levels for aquaporin channel genes AQP3 and AQP5 (Figure 4B). Additionally, there was a further significant down-regulation in the mRNA expression of occludin, a tight junction gene. The gap junction gene connexin43 also exhibited decreased mRNA expression, while the adhesion junction gene β-catenin showed a further significant down-regulation (Figure 4C). Furthermore, the expression of the peroxide gene, ptgs2, increased following knockdown of PKP2 (Figure 4D). The subsequent fluorescence yellow assay was conducted to measure endothelial cell permeability, revealing that PKP2 knockdown significantly increased endothelial cell permeability during acute inflammation (Figure 4E). The Rhodamine staining also revealed that the knockdown of PKP2 could exacerbate the disruption of F-actin morphology in LPS-stimulated living cell filaments (Figure 4F). Based on Western blot analysis, suppressing PKP2 was found to induce a decrease in the protein levels of ZO-1, β-catenin, and claudin1 in the context of acute inflammation (Figure 4G). The immunofluorescence Results supported the decreased expression of occludin following inhibition of PKP2 (Figure 4H). Altogether, these findings suggest that downregulation of PKP2 exacerbates the impairment of transcellular and paracellular pathways, as well as oxidative stress induced by acute inflammation.

Upregulation of PKP2 in Acute Inflammation Activates the p38/MAPK Signaling Pathway to Improve CLS

After LPS stimulation of HUVECs, WB detection showed that the p38/MAPK signaling pathway was inhibited, while the p38/MAPK signaling pathway was activated after PKP2 overexpression (Figure 5A). To confirm that the overexpression of PKP2 activates the p38/MAPK signaling pathway, LPS-stimulated cells were treated with SB203580, an inhibitor of this pathway. The rescue experiments demonstrated that SB203580 significantly attenuated the mRNA expression of connexin43, occludin, and ve-cadherin in HUVECs overexpressing PKP2 under LPS stimulation (Figure 5B). Furthermore, The Western blot experiments also demonstrated that SB203580 effectively suppressed the expression of ZO-1, β-catenin, p-p38/p38, and claudin1 proteins in HUVECs overexpressing PKP2 under LPS stimulation (Figure 5C). According to the immunofluorescence experiments, claudin1 expression decreased upon SB 203580 rescue (Figure 5D). Notably, the functional experiments demonstrated that SB203580 enhanced the permeability of LPS-stimulated endothelial cells overexpressing PKP2 (Figure 5E) and exacerbating cytoskeletal abnormalities (Figure 5F). These findings suggest improved capillary leakage via activation of the p38/MAPK signaling pathway by PKP2 overexpression.

Knocking Down PKP2 Depends on the Inhibition of the p38/MAPK Signaling Pathway for Increased CLS

In contrast, the p38/MAPK signaling pathway activator dehydrocorydaline was administered to interfere with the HUVECs of siPKP2 stimulated by LPS. The rescue experiment demonstrated that dehydrocorydaline treatment significantly enhanced the protein expression levels of ZO-1, β-catenin, occludin, and claudin1 in HUVECs with PKP2 knockdown under LPS stimulation (Figure 6A), and upregulated the mRNA expression of occludin and β-catenin (Figure 6B). In functional experiments, dehydrocorydaline rescue improved the endothelial cytoskeleton of PKP2 knockdown under LPS stimulation (Figure 6C) and reduced cell permeability (Figure 6D). These findings suggest that the downregulation of PKP2 exacerbates CLS by inhibiting the p38/MAPK signaling pathway.

Rosiglitazone, a PPARγ Activator, Targets the Upregulation of PKP2 to Inhibit Endothelial Cell Leakage

The PPARγ transcription factor upstream of PKP2 was predicted using the JASPAR, HumanTFDB, and GTRD databases. The PPARγ activator, rosiglitazone, was administered to the LPS-induced acute inflammatory endothelial

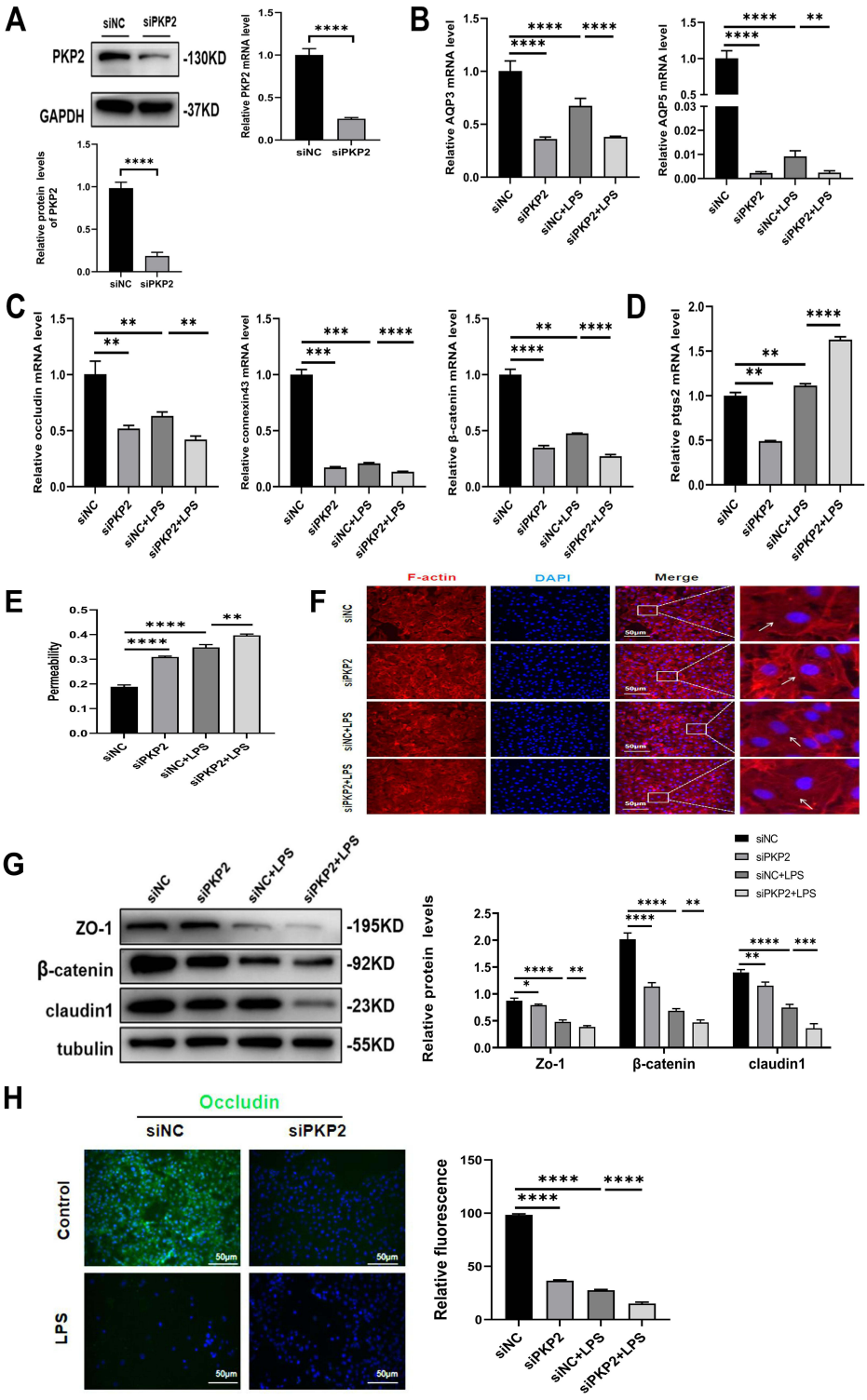

Figure 4 PKP2 knockdown regulates CLS during acute inflammation. (**A**) Successful verification of the PKP2 protein and mRNA knockdown (data represent three independent experiments). (**B**–**D**) The results of Lps-stimulated PKP2 knockdown in HUVECs demonstrated that down-regulation of PKP2 can significantly decrease the mRNA expression levels of CLS-related molecules, including AQP3, AQP5, occludin, connexin43, β-catenin, while simultaneously increasing the mRNA expression level of the oxidative stress-related gene ptgs2 (data represent the results of three independent experiments). (**E**) PKP2 knockdown resulted in increased permeability of HUVECs during acute inflammation (data represent the results of three independent experiments). (**F**) LPS-induced cytoskeleton disorder in HUVECs was aggravated after PKP2 knockdown (data represent the results of three independent experiments). (**G**) Decreased protein levels of ZO-1, β-catenin, and claudin1 were observed in HUVECs with acute inflammation after PKP2 knockdown (data represent the results of three independent experiments). (**H**) Immunofluorescence analysis revealed that occludin expression was downregulated in HUVECs with acute inflammation following PKP2 knockdown (data represent the results of three independent experiments). *p < 0.05, **p < 0.01, ***p < 0.001, ****p < 0.0001, ns p > 0.05.

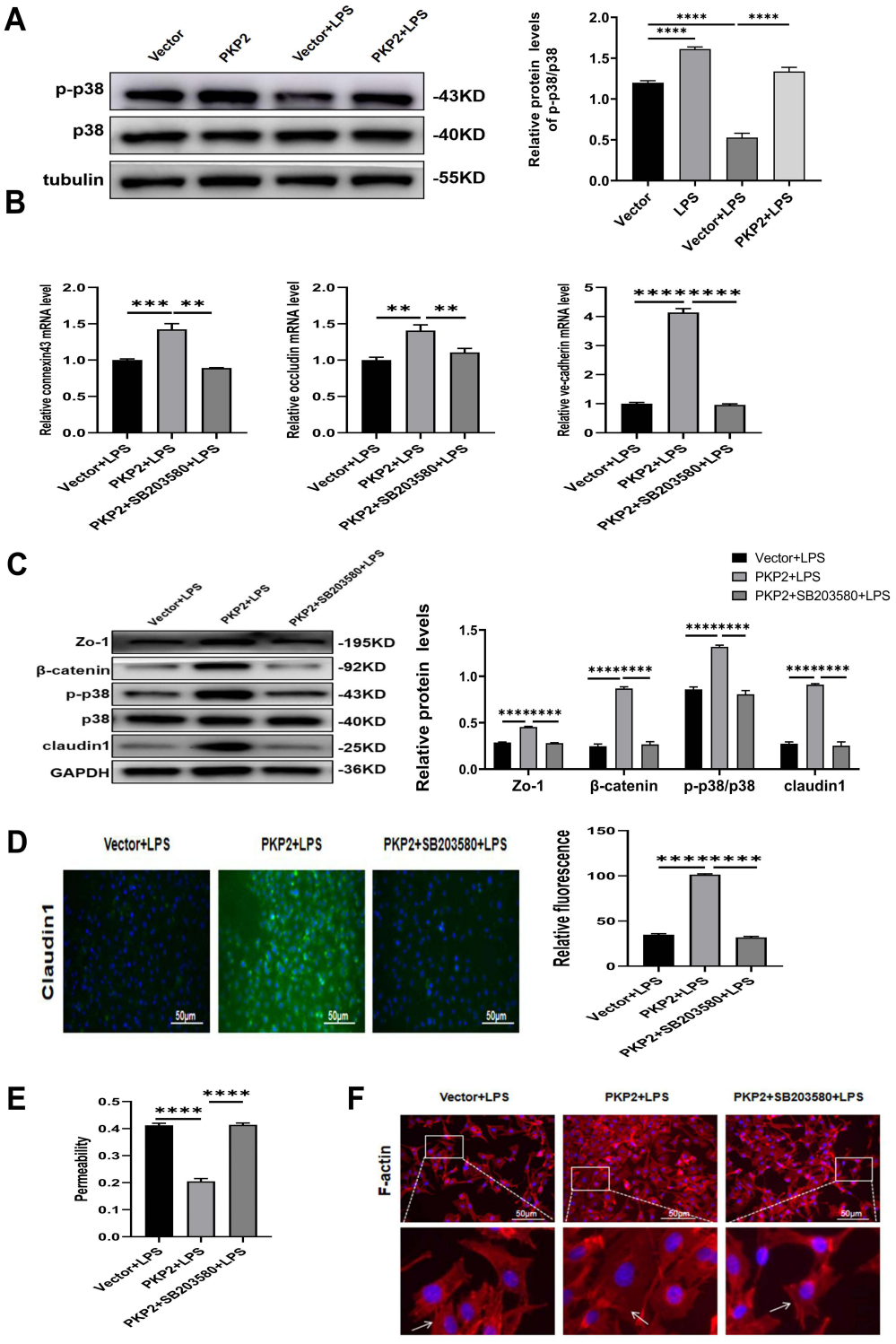

Figure 5 The overexpression of PKP2 in CLS, where acute inflammation occurs, triggers the activation of the p38/MAPK signaling pathway. (**A**) Western blot analysis revealed that PKP2 overexpression significantly increased the overall expression of phosphorylated p38 protein in HUVECs upon stimulation with LPS (data represent the results of three independent experiments). (**B**) Following LPS stimulation, SB203580 downregulated the mRNA expression levels of connexin43, occludin, and VE-cadherin in HUVECs with elevated PKP2 overexpression (data represent the results of three independent experiments). (**C**) Following LPS stimulation, SB203580 reduced the protein levels of ZO-1, β-catenin, p-p38/p38, and claudin1 in HUVECs overexpressing PKP2 (data represent the results of three independent experiments). The levels were compared to that of GAPDH, which served as the reference. (**D**) Immunofluorescence assay revealed that SB203580 downregulated claudin1 expression in LPS-treated PKP2 overexpressed HUVECs (data represent the results of three independent experiments). (**E**) SB203580 further decreased the permeability of PKP2 overexpressed HUVECs stimulated with LPS (data represent the results of three independent experiments). (**F**) SB203580 exacerbated cytoskeletal disorders induced by LPS treatment in PKP2 overexpressed HUVECs (data represent the results of three independent experiments). SB203580: Inhibitor of the p38/MAPK signaling pathway. **p < 0.01, ***p < 0.001, ****p < 0.0001, ns p > 0.05.

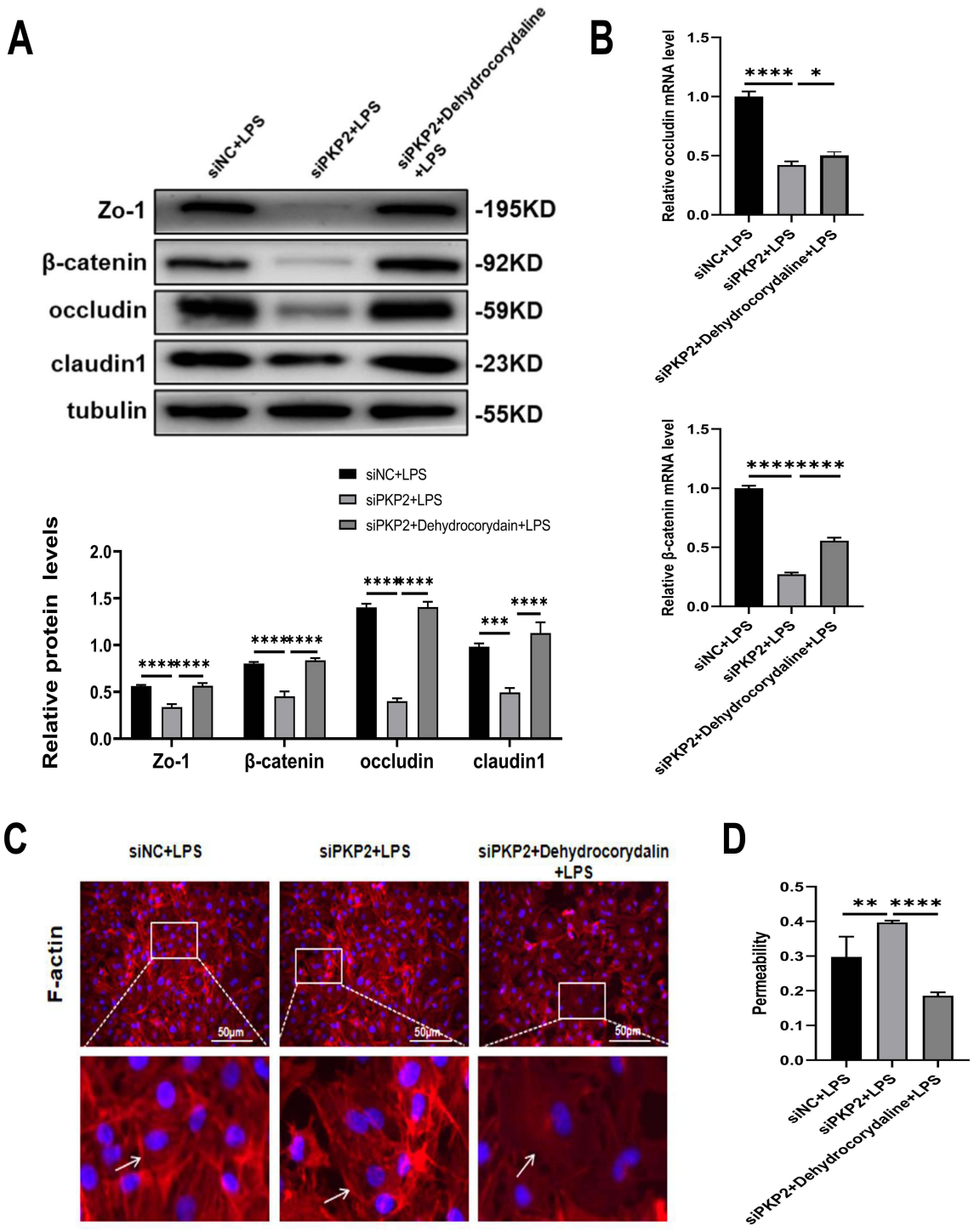

Figure 6 PKP2 knockdown increased endothelial cell leakage by inhibiting the p38/MAPK signaling pathway. (**A**) Following LPS stimulation, dehydrocorydaline upregulated the protein levels of ZO-1, β-catenin, occludin, and claudin1 in HUVECs with PKP2 knockdown according to Western blot analysis (data represent the results of three independent experiments). (**B**) Dehydrocorydaline increased the mRNA expression levels of occludin and β-catenin in HUVECs with PKP2 knockdown (data represent the results of three independent experiments). (**C**) Dehydrocorydaline improved the endothelial cytoskeleton morphology of PKP2 knockdown under LPS stimulation (data represent the results of three independent experiments). (**D**) Dehydrocorydaline reduced the permeability of HUVECs with PKP2 knockdown under LPS stimulation (data represent the results of three independent experiments). Dehydrocorydaline: Activator of the p38/MAPK signaling pathway. *p < 0.05, **p < 0.01, ***p < 0.001, ****p < 0.0001.

cell model. The Western blot experiment demonstrated a significant increase in the expression of PKP2, p-p38/p38, and claudin1 protein upon the addition of rosiglitazone. Moreover, rosiglitazone can target the up-regulation of PKP2 (Figure 7A). The mRNA expression of CLS-related genes AQP3 and occludin is up-regulated by rosiglitazone in

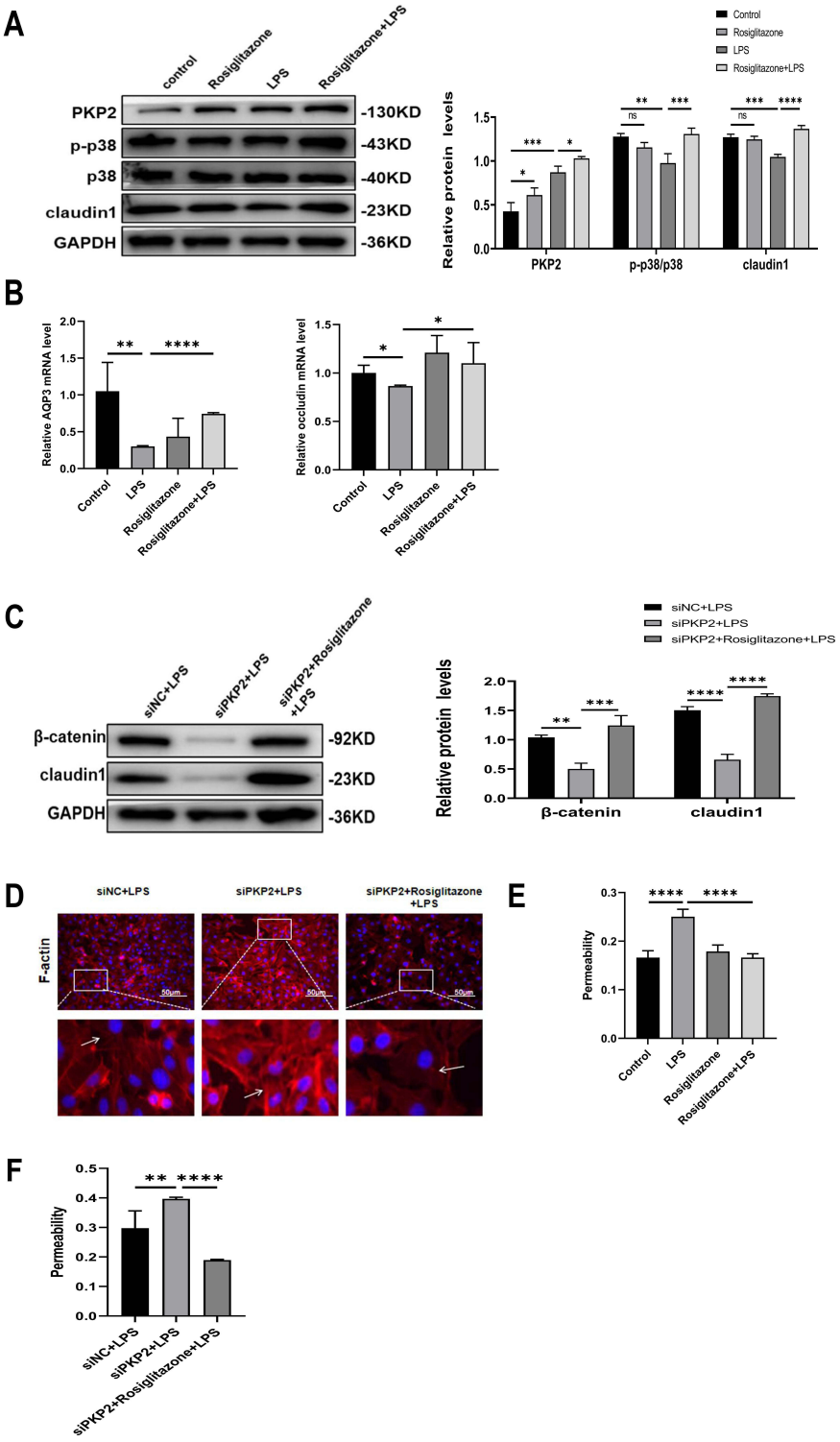

Figure 7 Rosiglitazone upregulates PKP2 and affects endothelial cell leakage. (**A**) Western blot analysis revealed that rosiglitazone markedly increased the expression levels of PKP2, p-p38/p38, and claudin1 proteins in HUVECs stimulated with LPS (data represent the results of three independent experiments). (**B**) Rosiglitazone significantly enhanced the mRNA expression of AQP3 and occludin in HUVECs stimulated with LPS (data represent the results of three independent experiments). (**C**) Following LPS stimulation, rosiglitazone significantly increased the protein expression of β-catenin and claudin1 in HUVECs with PKP2 knockdown (representative of three independent experiments). (**D**) Following LPS stimulation, the degree of porosity of the cytoskeleton in HUVECs with PKP2 knockdown was significantly improved by rosiglitazone (data represent the results of three independent experiments). (**E**) Rosiglitazone significantly decreased the permeability of HUVECs stimulated with LPS (data represent the results of three independent experiments). (**F**) Rosiglitazone significantly reduced the permeability of HUVECs with PKP2 knockdown upon LPS stimulation (data represent the results of three independent experiments). Rosiglitazone: agonist of PPARγ. *p < 0.05, **p < 0.01, ***p < 0.001, ****p <0.0001.

response to LPS stimulation (Figure 7B). According to the fluorescence yellow experiment, rosiglitazone decreased the permeability of endothelial cells during acute inflammation (Figure 7E). After PKP2 knockdown under LPS stimulation, WB results revealed a significant reduction in β-catenin and claudin1 protein levels in HUVECs. However, upon the addition of rosiglitazone, WB analysis demonstrated an increase in β-catenin and claudin1 protein levels in HUVECs (Figure 7C). In the functional rescue experiment, under LPS stimulation, rosiglitazone improved the endothelial cytoskeleton morphology of PKP2 knockdown (Figure 7D) and decreased endothelial cell permeability (Figure 7F). These findings indicate that rosiglitazone specifically acts on PKP2 to inhibit endothelial cell permeability.

Inhibition of the p38/MAPK Signaling Pathway by GW9662 Aggravates CLS

The PPARγ inhibitor, GW9662, was introduced into an LPS-induced acute inflammatory cell model. Based on Western blot analysis, the protein expression of PKP2 was downregulated, indicating that PKP2 is the target of inhibition (Figure 8A). Next, we carried out the rescue experiment. After overexpression of PKP2 endothelial cells stimulated by LPS, GW9662 down-regulated the mRNA expression of CLS-related genes connexin43 and AQP3 (Figure 8B). The results of the fluorescence yellow test demonstrated that GW9662 significantly enhanced the permeability of HUVECs under LPS stimulation (Figure 8C). The subsequent rescue experiment was conducted, wherein the Western blot results demonstrated that GW9662 exhibited a down-regulatory effect on the protein levels of ZO-1 and claudin1 in HUVECs overexpressing PKP2 after LPS stimulation (Figure 8C). Additionally, there was a notable decrease observed in the p-p38/p38 protein ratio (Figure 8C). The functional rescue experiment revealed that GW9662 when stimulated by LPS, exacerbated the cytoskeletal morphological disorder caused by PKP2 overexpression (Figure 8D) and increased endothelial cell permeability (Figure 8E). Immunofluorescence assay showed that GW9662 down-regulated claudin1 expression in LPS-stimulated HUVECs that overexpressed PKP2 (Figure 8F). These findings suggest that targeting PKP2 with GW9662 enhances endothelial cell leakage.

Discussion

AP is one of the most prevalent inflammatory diseases affecting the digestive system, with approximately 20% of patients experiencing SAP.[36] SAP often leads to pancreatic necrosis, systemic inflammatory response syndrome, and multiple organ dysfunction and failure, resulting in high mortality rates and ineffective treatment options.[4] CLS represents an intermediate stage between the systemic inflammatory response syndrome and MOF in SAP. Therefore, studying the pathogenesis of CLS is crucial for effective management of SAP. The expression of PKP2 in SAP has been demonstrated to be significantly elevated based on research findings.[37] In this study, we observed the protective upregulation of PKP2 in SAP. Notably, the exogenous elevation of PKP2 can upregulate molecules associated with CLS under inflammatory stimulation. The overexpression of PKP2 activated the p38/MAPK signaling pathway and the administration of rosiglitazone enhanced PKP2 expression to reduce inflammation and protect against SAP progression. Overall, our findings highlight the potential of PKP2 to ameliorate CLS induced by SAP and the novel mechanism underlying its development.

CLS in SAP can increase the permeability of endothelial cells throughout the body, resulting in the leakage of plasma proteins from blood capillaries, thereby decreasing colloid osmotic pressure. Consequently, insufficient absorption of tissue fluid and an aberrant build-up of fluid occur, which lead to the development of various organ dysfunction.[38] Following the onset of CLS in SAP, capillary endothelial dysfunction leads to the activation and dissemination of inflammatory cells and factors. The upregulation of intercellular adhesion molecule, platelet endothelial cell adhesion molecule 1, and endothelial leukocyte adhesion molecule 1 enhances the rolling of white blood cells, ultimately worsening the systemic inflammatory response. As a result, the cascade activation of pancreatic enzymes leads to an increase in pancreatic necrosis, sustained damage to capillary endothelial cells, the establishment of a vicious cycle, and ultimately results in multiple organ failure.[7,39] Yin et al discovered a reduction in pancreatic microvasoconstriction and blood distribution patterns in mice with cerulein- and LPS-induced AP. However, the administration of angiotensin-(1-7) could restore pancreatic microcirculation function.[40] Two years later, these investigators further explored this phenomenon and found that angiotensin-(1-7) exerts its effects by targeting telomerase reverse transcriptase, inhibiting the production of mitochondrial reactive oxygen species, alleviating mitochondrial dysfunction, and reducing endothelial cell

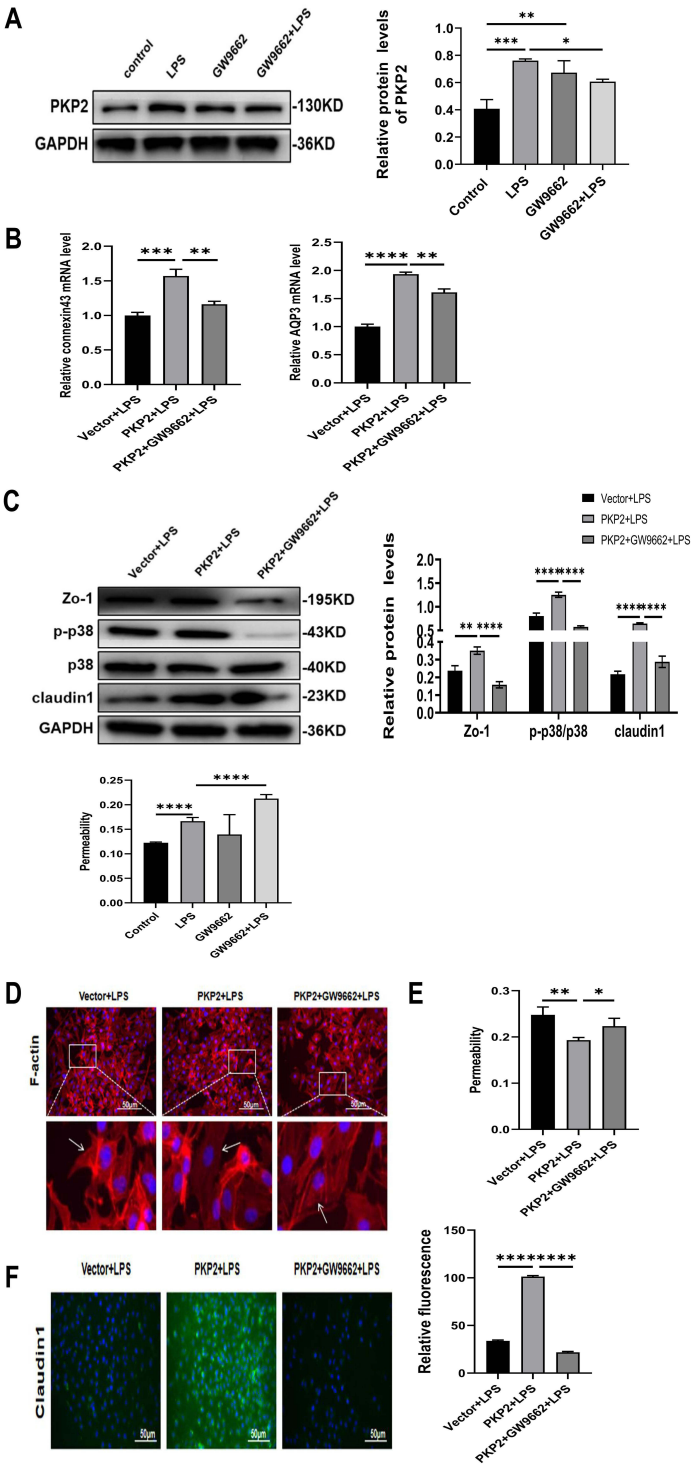

Figure 8 Targeting PKP2 using GW9662 leads to the downregulation of the P38/MAPK signaling pathway. (**A**) Western blot analysis revealed that GW9662 markedly reduced the production of the PKP2 protein in HUVECs stimulated with LPS (data represent the results of three independent experiments). (**B**) GW9662 significantly reduced the mRNA expression of connexin43 and AQP3 in HUVECs overexpressing PKP2 upon LPS stimulation (data represent the results of three independent experiments). (**C**) In the presence of LPS, GW9662 substantially reduced the protein levels of ZO-1, p-p38/p38, and claudin1 in HUVECs overexpressing PKP2 and simultaneously enhanced cell permeability (data represent the results of three independent experiments). (**D**) After LPS stimulation, GW9662 induced cytoskeletal disruption in HUVECs overexpressing PKP2 (data represent the results of three independent experiments). (**E**) GW9662 increased the permeability of HUVECs overexpressing PKP2 upon LPS stimulation (data represent the results of three independent experiments). (**F**) GW9662 decreased the immunofluorescence intensity of claudin1 in HUVECs overexpressing PKP2 following LPS stimulation (data represent the results of three independent experiments). GW9662: antagonist of PPARγ. *p < 0.05, **p < 0.01, ***p < 0.001, ****p <0.0001.

permeability. Consequently, pancreatic microcirculation function was found to be successfully restored.[41] Consistent with these findings, cerulein and LPS were administered intraperitoneally to generate a model of SAP. Notable increases were found in the levels of serum lipase, amylase, IL-6, TNF-α, and IL-1β. In addition, the permeability of endothelial cells was significantly increased in both pancreatic and lung tissues compared to wild-type mice. Furthermore, notable increases in the wet and dry weights of pancreatic and lung tissues were recorded a, suggesting the existence of capillary leakage syndrome in these organs. Yang et al[42] found that the decrease and altered distribution of ZO-1, a protein that forms tight junctions in vascular endothelial cells, induce an increase in the permeability of endothelial cells. As a result, neutrophils and monocytes can more easily enter the cells, causing inflammation in the blood vessels. Consistent with the findings of previous studies, the levels of ZO-1, occludin, and VE-cadherin were found to be decreased in the pancreatic tissue of SAP mice. Transcriptome sequencing and bioinformatics analysis also revealed a notable increase in the expression of PKP2. Further studies are needed to determine the involvement of PKP2 in the etiology of CLS in SAP and its functional importance.

The roles of PKP2 in inflammation are complex and vary according to specific conditions. Recent findings revealed that during tumor advancement, epidermal growth factor receptor (EGFR) attracts PKP2 to the plasma membrane, ultimately inducing the activation of the E3 ubiquitin ligase, HOIP, which is associated with the EGFR complex. Consequently, nuclear transcription factor-κB (NF-κB) is activated by i-κB phosphorylation.[43] Subsequent studies revealed a notable reduction in the mRNA expression levels of PKP2 in patients with chronic periodontitis compared to control individuals. In this process, porphyromonas (*P*) *gingivalis* breaks down the PKP2 protein through cysteine protease, which compromises gingival epithelial barrier function and induces the onset of periodontitis.[44] Conversely, we noted a substantial increase in PKP2 levels in the pancreatic tissue of mice with SAP, suggesting that PKP2 may play a vital role in enhancing defense mechanisms during the initial phase of CLS in SAP. As expected, our findings clearly demonstrate the beneficial effects of PKP2, including its capacity to decrease the permeability of endothelial cells and maintain the microstructure of cytoskeletal. According to prior studies, PKP2 regulates the tight junction proteins, claudin1 and claudin4, through protein kinase C, consequently supporting the integrity of intestinal barrier function.[45] Furthermore, suppressing PKP2 was found to induce the inhibition of mouse embryo implantation via a decrease in the production of connexin 43, which weakens communication between cells through gap junctions.[46] In addition, PKP2, a desmosomal connexin, was not found to exist independently. PKP2 creates "meningeal junctions" by interacting with traditional endothelial adhesion proteins, such as E-cadherin (or N-cadherin), α-catenin, β-catenin, and others, as found in human meningioma cells.[47] In contrast to prior findings, PKP2 overexpression can reverse the decrease in ZO-1, claudin1, and β-catenin caused by LPS; however, PKP2 knock-down accelerates the decrease in ZO-1, occludin, claudin1, and β-catenin. The expression of PKP2 was significantly up-regulated in CLS in SAP, which was inconsistent with common sense and should be down-regulated. Elevated capillary permeability and decreased molecular expression are hypothesized to occur after the development of CLS in SAP. Contrary to our previous research, Contrary to our previous research, PKP2 expression should also be down-regulated, which aggravates the progression of CLS and ultimately leads to MOF. Nevertheless, we observed a notable increase in PKP2 expression. As a result, we hypothesized that PKP2 has a crucial protective function in the initial phase of CLS in SAP by strengthening the cytoskeleton and decreasing the permeability of endothelial cells. Additional validation using animal experiments is required. This is because SAP will have the same MOF outcome after experiencing CLS. The early stage upregulation of PKP2 expression triggers a defensive reaction in the body, whereas its protective impact at later stages remains uncertain. Hence, increased PKP2 expression is highly significant in the treatment of early-stage CLS in SAP.

Dysiarenone blocks the anti-inflammatory effects of the NF-κB signaling pathway by impeding the phosphorylation of p65 and p38 in LPS-stimulated RAW 264.7 macrophages.[48] According to Xia et al,[49] activation of the p38/MAPK signaling pathway might attract inflammatory cells, such as T cells and neutrophils. Conversely, suppressing p38 phosphorylation helps relieve chronic inflammatory illnesses.[50,51] The p38/MAPK signaling pathway is linked to both acute and chronic inflammatory disorders. Zhu et al[52] discovered that suppressing the activity of thioredoxin-interacting proteins has a beneficial effect in reducing inflammation and oxidative stress by blocking the ASK1-dependent JNK/p38 signaling pathway. To prevent SAP and the resulting damage to the lungs and kidneys, Xue et al examined the effect of SB203580, a p38 MAPK inhibitor, on SAP. Based on their findings, inhibiting the p38/MAPK signaling pathway could

effectively protect against SAP-induced acute lung injury by reducing damage to the pulmonary microvascular endothelium.[53] LPS-induced acute inflammation in HUVECs led to a decrease in p38 phosphorylation and inhibition of the p38/MAPK signaling pathway. Nevertheless, the overexpression of PKP2 restored the amount of p38 phosphorylation. Next, we verified that PKP2 regulates endothelial cell permeability and paracellular pathway molecules by activating the p38/MAPK signaling pathway. SB203580 reversed the decreasing effect of up-regulated PKP2 on endothelial cell permeability, while p38/MAPK agonists eliminated the increasing effect of down-regulated PKP2 on endothelial cell permeability. SB203580 counteracted the elevated levels of PKP2, which resulted in decreased endothelial cell permeability. Conversely, p38 MAPK agonists nullified this reduction in PKP2 expression, leading to an increase in endothelial cell permeability. Moreover, overexpression of PKP2 and the addition of SB203580 can eliminate upregulation of ZO-1, claudin1, and β-catenin. These findings indicate that PKP2 can increase the expression of ZO-1, claudin1, and β-catenin through the p38/MAPK signaling pathway, leading to enhanced permeability of endothelial cells. Overall, directing efforts toward PKP2 could serve as a promising therapeutic approach for SAP-related CLS. Based on our database analysis, PPARγ is predicted to function as a transcription factor in the regulation of PKP2.

Prophylactic administration of the PPARγ agonist, rosiglitazone, after endoscopic retrograde cholangiopancreatography exhibited a protective effect in rat models of acute pancreatitis. Similarly, rosiglitazone exerted a protective effect in a rat model of cerulein-induced acute pancreatitis by downregulating miR-26a and upregulating PTEN to inhibit the PI3K/AKT signaling pathway, thereby exerting an anti-inflammatory effect.[54] Although the administration of rosiglitazone did not reduce the severity of acute pancreatitis in obese mice after intraperitoneal injection of IL-12+IL-18, prophylactic or concurrent administration of rosiglitazone improved AP.[55] In this study, the PPARγ activator, rosiglitazone, was administered as a preventive measure, and then HUVECs were stimulated with LPS. As a result, PKP2 expression markedly increased and the decrease in claudin1 and β-catenin levels was reversed. In contrast, the suppression of PPARγ by GW9662 notably intensified the decrease in ZO-1 and claudin1, resulting in increased permeability of endothelial cells. Rosiglitazone, an activator of PPARγ, can upregulate PKP2, a new target, to protect CLS.

Currently, there is no existing literature reporting the role of PPARγ-targeted up-regulation of PKP2 in SAP. However, relevant literature has documented the involvement of PPARγ in AP treatment. The recent proposal of new insights suggests that emodin exhibits potential in the treatment of SAP rats, as it effectively reduces plasma exosomes and mitigates lung injury associated with SAP by activating PPARγ to inhibit NF-kB pathways.[56] Similarly, it has been proposed that the upregulation of PPARγ levels can facilitate the polarization of alveolar macrophages from an M1 phenotype to an M2 phenotype, thereby attenuating the severity of lung injury associated with acute pancreatitis.[57] Furthermore, PPARγ suppresses NF-kB activity to attenuate Cerulein-induced inflammation in pancreatic acinar AR42J cells.[58] The reduction of PPARγ-coactivator 1 (PGC-1) in AP leads to a decrease in its binding affinity with p65 in NFkB, resulting in an augmentation of IL-6-mediated inflammatory damage.[59] Additionally, PPARγ is implicated in cell junctions. The activation of PPARγ by prostaglandin D2 metabolite in acute pancreatitis can attenuate the expression of intercellular adhesion molecule-1, thereby mitigating the severity of the condition.[60] In conclusion, there is evidence to suggest that PPARγ is associated with AP, and potentially even with CLS in SAP. This study exclusively examined in vitro investigations where the PPARγ activator rosiglitazone targeted PKP2 to mitigate inflammation in LPS-stimulated HUVECs. The next step of our research will involve investigating the in vivo mechanism of action for both PPARγ and PKP2 in SAP disease.

In summary, PKP2 was identified as a novel and effective early protective molecule against SAP. PKP2 effectively decreased the permeability of endothelial cells and increased the expression of intercellular junction molecules by activating phosphorylation of the p38/MAPK signaling pathway. These compelling data fundamentally transform our understanding of the function of PKP2 in safeguarding against SAP. Therefore, the increase in PKP2 induced by rosiglitazone and modulation of the p38/MAPK signaling pathway may offer a potential strategy to improve SAP-related CLS. Exogenously increasing PKP2 expression is a promising novel treatment approach for CLS in SAP. Nevertheless, the specific constraints inherent to this study must be highlighted. First, the mechanisms discussed in this study have not been confirmed via animal experiments or in individuals with SAP. Further studies are also needed to clarify the internal mechanism by which PKP2 depends on the

p38/MAPK signaling pathway to protect against CLS in SAP. These discoveries may promote clinical research, whether prospective or retrospective, to increase the therapeutic options for SAP.

Data Sharing Statement

Data supporting the findings of this study can be found in the Supplementary Material. The datasets generated or analyzed in this study are available from the corresponding authors upon reasonable request.

Ethical Approval

All laboratory operations on Animals follow the Guidelines for the Care and Use of Laboratory Animals published by the National Research Council and published by the National Institutes of Health. This study was approved by the Institutional Ethics Review Committee of Longhua District People's Hospital, Shenzhen (No. 2309013).

Acknowledgments

This study was financially supported by the Medical Research Project of the Longhua District Medical Association of Shenzhen (No. 2023LHMA06).

Author Contributions

Liu PI supervised the study; Liu Hui oversaw the design of the experiments, conducted the experiments, analyzed the data, and produced the report; Li Ji and Xu Xuan performed the literature search and conducted cell culture; Zheyu Liu and Yuwen Xiong conducted the bioinformatics analysis; and Yue Mengli conducted the cell transfection experiments. All authors made a significant contribution to the work, whether in its conception, study design, execution, acquisition of data, analysis, and interpretation, or all areas; participated in drafting, revising, or critically reviewing the article; gave final approval of the version to be published; agreed on the journal for article submission; and agreed to be accountable for all aspects of the work.

Disclosure

The authors declare no conflicts of interest in this work.

References

1. Mederos MA, Reber HA, Girgis MD. Acute pancreatitis: a review. *JAMA*. 2021;325(4):382–390. doi:10.1001/jama.2020.20317
2. Szatmary P, Grammatikopoulos T, Cai W, et al. Acute pancreatitis: diagnosis and treatment. *Drugs*. 2022;82(12):1251–1276. doi:10.1007/s40265-022-01766-4
3. Mofidi R, Duff MD, Wigmore SJ, Madhavan KK, Garden OJ, Parks RW. Association between early systemic inflammatory response, severity of multiorgan dysfunction and death in acute pancreatitis. *Br J Surg*. 2006;93(6):738–744. doi:10.1002/bjs.5290
4. Schepers NJ, Bakker OJ, Besselink MG, et al. Impact of characteristics of organ failure and infected necrosis on mortality in necrotising pancreatitis. *Gut*. 2019;68(6):1044–1051. doi:10.1136/gutjnl-2017-314657
5. Boxhoorn L, Voermans RP, Bouwense SA, et al. Acute pancreatitis. *Lancet*. 2020;396(10252):726–734. doi:10.1016/S0140-6736(20)31310-6
6. Gliem N, Ammer-Herrmenau C, Ellenrieder V, Neesse A. Management of severe acute pancreatitis: an update. *Digestion*. 2021;102(4):503–507. doi:10.1159/000506830
7. Cuthbertson CM, Christophi C. Disturbances of the microcirculation in acute pancreatitis. *Br J Surg*. 2006;93(5):518–530. doi:10.1002/bjs.5316
8. Sukriti S, Tauseef M, Yazbeck P, Mehta D. Mechanisms regulating endothelial permeability. *Pulm Circ*. 2014;4(4):535–551. doi:10.1086/677356
9. Ghim M, Alpresa P, Yang SW, et al. Visualization of three pathways for macromolecule transport across cultured endothelium and their modification by flow. *Am J Physiol Heart Circulatory Physiol*. 2017;313(5):H959–h973. doi:10.1152/ajpheart.00218.2017
10. Eibl G, Buhr HJ, Foitzik T. Therapy of microcirculatory disorders in severe acute pancreatitis: what mediators should we block? *Intensive Care Med*. 2002;28(2):139–146. doi:10.1007/s00134-001-1194-1
11. Choi HJ, Weis WI. Structure of the armadillo repeat domain of plakophilin 1. *J Mol Biol*. 2005;346(1):367–376. doi:10.1016/j.jmb.2004.11.048
12. Cerrone M, Marrón-Liñares GM, van Opbergen CJM, et al. Role of plakophilin-2 expression on exercise-related progression of arrhythmogenic right ventricular cardiomyopathy: a translational study. *Eur Heart J*. 2022;43(12):1251–1264. doi:10.1093/eurheartj/ehab772
13. Corrado D, Link MS, Calkins H. Arrhythmogenic right ventricular cardiomyopathy. *New Engl J Med*. 2017;376(1):61–72. doi:10.1056/NEJMra1509267
14. Austin KM, Trembley MA, Chandler SF, et al. Molecular mechanisms of arrhythmogenic cardiomyopathy. *Nat Rev Cardiol*. 2019;16(9):519–537. doi:10.1038/s41569-019-0200-7

15. Pérez-Hernández M, van Opbergen CJM, Bagwan N, et al. Loss of nuclear envelope integrity and increased oxidant production cause DNA damage in adult hearts deficient in PKP2: a molecular substrate of ARVC. *Circulation*. 2022;146(11):851–867. doi:10.1161/CIRCULATIONAHA.122.060454
16. Pérez-Hernández M, Marrón-Liñares GM, Schlamp F, et al. Transcriptomic coupling of PKP2 with inflammatory and immune pathways endogenous to adult cardiac myocytes. *Front Physiol*. 2020;11:623190. doi:10.3389/fphys.2020.623190
17. Li MW, Mruk DD, Lee WM, Cheng CY. Connexin 43 and plakophilin-2 as a protein complex that regulates blood-testis barrier dynamics. *Proc Natl Acad Sci USA*. 2009;106(25):10213–10218. doi:10.1073/pnas.0901700106
18. Koetsier JL, Amargo EV, Todorović V, Green KJ, Godsel LM. Plakophilin 2 affects cell migration by modulating focal adhesion dynamics and integrin protein expression. *J Invest Dermatol*. 2014;134(1):112–122. doi:10.1038/jid.2013.266
19. Dubash AD, Kam CY, Aguado BA, et al. Plakophilin-2 loss promotes TGF-β1/p38 MAPK-dependent fibrotic gene expression in cardiomyocytes. *J Cell Biol*. 2016;212(4):425–438. doi:10.1083/jcb.201507018
20. Luan J, Kou J, Huang N, et al. Inhibition of CHRM3 alleviates necrosis via the MAPK-p38/miR-31-5p/RIP3 axis in l-arginine-induced severe acute pancreatitis. *Pancreas*. 2020;49(10):1335–1341. doi:10.1097/MPA.0000000000001684
21. Wettschureck N, Strilic B, Offermanns S. Passing the vascular barrier: endothelial signaling processes controlling extravasation. *Physiol Rev*. 2019;99(3):1467–1525. doi:10.1152/physrev.00037.2018
22. Claesson-Welsh L, Dejana E, McDonald DM. Permeability of the endothelial barrier: identifying and reconciling controversies. *Trends Mol Med*. 2021;27(4):314–331. doi:10.1016/j.molmed.2020.11.006
23. Zeng X, He G, Yang X, et al. Zebularine protects against blood-brain-barrier (BBB) disruption through increasing the expression of zona occludens-1 (ZO-1) and vascular endothelial (VE)-cadherin. *Bioengineered*. 2022;13(2):4441–4454. doi:10.1080/21655979.2021.2024323
24. Wautier JL, Wautier MP. Vascular permeability in diseases. *Int J Mol Sci*. 2022;23(7):3645. doi:10.3390/ijms23073645
25. Chen DQ, Shen MJ, Wang H, et al. Sirt3 maintains microvascular endothelial adherens junction integrity to alleviate sepsis-induced lung inflammation by modulating the interaction of VE-cadherin and β-catenin. *Oxid Med Cell Longev*. 2021;2021:8978795. doi:10.1155/2021/8978795
26. Jindal S, Chockalingam S, Ghosh SS, Packirisamy G. Connexin and gap junctions: perspectives from biology to nanotechnology based therapeutics. *Transl Res*. 2021;235:144–167. doi:10.1016/j.trsl.2021.02.008
27. Zhao H, Kong H, Wang W, et al. High glucose aggravates retinal endothelial cell dysfunction by activating the RhoA/ROCK1/pMLC/Connexin43 signaling pathway. *Invest Ophthalmol Visual Sci*. 2022;63(8):22. doi:10.1167/iovs.63.8.22
28. Masamune A, Suzuki N, Kikuta K, et al. Connexins regulate cell functions in pancreatic stellate cells. *Pancreas*. 2013;42(2):308–316. doi:10.1097/MPA.0b013e31825c51d6
29. Zhang J, Wang P, Wu Y, et al. Role of AQP3 in the vascular leakage of sepsis and the protective effect of Ss-31. *J Cardiovasc Pharmacol*. 2021;78(2):280–287. doi:10.1097/FJC.0000000000001050
30. Jiang Y, Ma R, Zhao Y, et al. MEF2C/miR-133a-3p.1 circuit-stabilized AQP1 expression maintains endothelial water homeostasis. *FEBS Lett*. 2019;593(18):2566–2573. doi:10.1002/1873-3468.13516
31. Jiang A, Zhang Y, Zhang X, et al. Morin alleviates LPS-induced mastitis by inhibiting the PI3K/AKT, MAPK, NF-κB and NLRP3 signaling pathway and protecting the integrity of blood-milk barrier. *Int Immunopharmacol*. 2020;78:105972. doi:10.1016/j.intimp.2019.105972
32. Zhang B, Wei X, Ding M, Luo Z, Tan X, Zheng Z. Daidzein protects Caco-2 cells against lipopolysaccharide-induced intestinal epithelial barrier injury by suppressing PI3K/AKT and P38 pathways. *Molecules*. 2022;27(24):8928. doi:10.3390/molecules27248928
33. Yang J, Zhang JN, Chen WL, et al. Effects of AQP5 gene silencing on proliferation, migration and apoptosis of human glioma cells through regulating EGFR/ERK/ p38 MAPK signaling pathway. *Oncotarget*. 2017;8(24):38444–38455. doi:10.18632/oncotarget.16461
34. Ma X, Dong X, Xu Y, et al. Identification of AP-1 as a critical regulator of glutathione peroxidase 4 (GPX4) transcriptional suppression and acinar cell ferroptosis in acute pancreatitis. *Antioxidants*. 2022;12(1):100. doi:10.3390/antiox12010100
35. Qiang Z, Dong H, Xia Y, Chai D, Hu R, Jiang H. Nrf2 and STAT3 alleviates ferroptosis-mediated IIR-ALI by regulating SLC7A11. *Oxid Med Cell Longev*. 2020;2020:5146982. doi:10.1155/2020/5146982
36. Garg PK, Madan K, Pande GK, et al. Association of extent and infection of pancreatic necrosis with organ failure and death in acute necrotizing pancreatitis. *Clin Gastroenterol Hepatol*. 2005;3(2):159–166. doi:10.1016/S1542-3565(04)00665-2
37. Glaubitz J, Wilden A, Frost F, et al. Activated regulatory T-cells promote duodenal bacterial translocation into necrotic areas in severe acute pancreatitis. *Gut*. 2023;72(7):1355–1369. doi:10.1136/gutjnl-2022-327448
38. Komara NL, Paragomi P, Greer PJ, et al. Severe acute pancreatitis: capillary permeability model linking systemic inflammation to multiorgan failure. *Am J Physiol Gastrointest Liver Physiol*. 2020;319(5):G573–g583. doi:10.1152/ajpgi.00285.2020
39. Zhou ZG, Chen YD. Influencing factors of pancreatic microcirculatory impairment in acute pancreatitis. *World J Gastroenterol*. 2002;8(3):406–412. doi:10.3748/wjg.v8.i3.406
40. Wang X, Liu M, Hu W, et al. Angiotensin-(1-7) treatment restores pancreatic microcirculation profiles: a new story in acute pancreatitis. *Pancreas*. 2020;49(7):960–966. doi:10.1097/MPA.0000000000001609
41. Wang X, Cui T, Zhang T, Hu W, Liu R, Yin C. Angiotensin-(1-7) restores microcirculation profiles in acute pancreatitis: secret of telomerase reverse transcriptase. *Pancreas*. 2022;51(8):1047–1055. doi:10.1097/MPA.0000000000002139
42. Yang X, Xu C, Yao F, et al. Targeting endothelial tight junctions to predict and protect thoracic aortic aneurysm and dissection. *Eur Heart J*. 2023;44(14):1248–1261. doi:10.1093/eurheartj/ehac823
43. Hua F, Hao W, Wang L, Li S. Linear ubiquitination mediates EGFR-induced NF-κB pathway and tumor development. *Int J Mol Sci*. 2021;22(21):11875. doi:10.3390/ijms222111875
44. Yu N, Zhang J, Phillips ST, Offenbacher S, Zhang S. Impaired function of epithelial plakophilin-2 is associated with periodontal disease. *J Periodontal Res*. 2021;56(6):1046–1057. doi:10.1111/jre.12918
45. Nagler S, Ghoreishi Y, Kollmann C, et al. Plakophilin 2 regulates intestinal barrier function by modulating protein kinase C activity in vitro. *Tissue Barriers*. 2022;11(4):2138061. doi:10.1080/21688370.2022.2138061
46. Sugimoto M, Sasaki S, Gotoh Y, et al. Genetic variants related to gap junctions and hormone secretion influence conception rates in cows. *Proc Natl Acad Sci USA*. 2013;110(48):19495–19500. doi:10.1073/pnas.1309307110
47. Akat K, Bleck CK, Lee YM, Haselmann-Weiss U, Kartenbeck J. Characterization of a novel type of adherens junction in meningiomas and the derived cell line HBL-52. *Cell Tissue Res*. 2008;331(2):401–412. doi:10.1007/s00441-007-0512-5

48. Hu TY, Zhang H, Chen YY, et al. Dysiarenone from marine sponge dysidea arenaria attenuates ROS and inflammation via Inhibition of 5-LOX/NF-κB/MAPKs and Upregulation of Nrf-2/OH-1 in RAW 264.7 Macrophages. *J Inflamm Res*. 2021;14:587–597. doi:10.2147/JIR.S283745
49. Ren K, Xia Y. Lipocalin 2 participates in the epidermal differentiation and inflammatory processes of psoriasis. *J Inflamm Res*. 2022;15:2157–2166. doi:10.2147/JIR.S358492
50. Li B, Yang X, Zhang P, et al. Engeletin alleviates the inflammation and apoptosis in intervertebral disc degeneration via inhibiting the NF-κB and MAPK pathways. *J Inflamm Res*. 2022;15:5767–5783. doi:10.2147/JIR.S371809
51. Lo J, Liu CC, Li YS, et al. Punicalagin attenuates LPS-induced inflammation and ROS production in microglia by inhibiting the MAPK/NF-κB signaling pathway and NLRP3 inflammasome activation. *J Inflamm Res*. 2022;15:5347–5359. doi:10.2147/JIR.S372773
52. Liu Y, Li M, Mei C, et al. Thioredoxin-interacting protein deficiency protects against severe acute pancreatitis by suppressing apoptosis signal-regulating kinase 1. *Cell Death Dis*. 2022;13(10):914. doi:10.1038/s41419-022-05355-x
53. Zhang XX, Wang HY, Yang XF, et al. Alleviation of acute pancreatitis-associated lung injury by inhibiting the p38 mitogen-activated protein kinase pathway in pulmonary microvascular endothelial cells. *World J Gastroenterol*. 2021;27(18):2141–2159. doi:10.3748/wjg.v27.i18.2141
54. Chen Y, Xiang W, Li X, Wang D, Qian C. Rosiglitazone prevents acute pancreatitis through inhibiting microRNA-26a expression. *Exp Ther Med*. 2019;18(2):1246–1252. doi:10.3892/etm.2019.7711
55. Malecki EA, Castellanos KJ, Cabay RJ, Fantuzzi G. Therapeutic administration of orlistat, rosiglitazone, or the chemokine receptor antagonist RS102895 fails to improve the severity of acute pancreatitis in obese mice. *Pancreas*. 2014;43(6):903–908. doi:10.1097/MPA.0000000000000115
56. Hu Q, Yao J, Wu X, et al. Emodin attenuates severe acute pancreatitis-associated acute lung injury by suppressing pancreatic exosome-mediated alveolar macrophage activation. *Acta Pharm Sin B*. 2022;12(10):3986–4003. doi:10.1016/j.apsb.2021.10.008
57. Ding F, Liu G, Gao F, et al. Adropin attenuates pancreatitis-associated lung injury through PPARγ phosphorylation-related macrophage polarization. *Int J Mol Med*. 2023;52(4). doi:10.3892/ijmm.2023.5298
58. Wan H, Yuan Y, Qian A, Sun Y, Qiao M. Pioglitazone, a PPARgamma ligand, suppresses NFkappaB activation through inhibition of IkappaB kinase activation in cerulein-treated AR42J cells. *Biomed Pharmacother*. 2008;62(7):466–472. doi:10.1016/j.biopha.2007.10.012
59. Diakopoulos KN, Algül H. New wine into old wineskins: PGC-1α and NF-κB in obesity and acute pancreatitis. *J Pathol*. 2019;248(1):6–8. doi:10.1002/path.5220
60. Hashimoto K, Ethridge RT, Saito H, Rajaraman S, Evers BM. The PPARgamma ligand, 15d-PGJ2, attenuates the severity of cerulein-induced acute pancreatitis. *Pancreas*. 2003;27(1):58–66. doi:10.1097/00006676-200307000-00009